Gravitational wave imprints of the doublet left-right symmetric model[a]

Dhruv Ringe, IIT Indore

PHOENIX-2023

20 December 2023

[a] arxiv: 2309.12023, with Siddhartha Karmakar (TIFR, IITB)

Motivation

Gravitational Wave Astronomy

- 1^{st} direct detection: BH-BH merger by LIGO/VIRGO in 2015, ~ 50 detections as of December 2019.
- 2023, (possible) detection of nanoHz GW background by PTAs.
- Cosmological sources of GW background: inflation, domain walls, cosmic strings, first-order phase transitions.
- Planned: aLIGO, LISA, ET, BBO, DECIGO, CE, SKA.
- Fresh look at the universe!

Phase transitions in particle physics

- Particle physics model featuring spontaneous symmetry breaking:

$$G \xrightarrow{v \neq 0} H.$$

- At temperature T, the *vev* $(v \equiv \langle \phi \rangle)$ lies at the minimum of the effective potential, $V_{\text{eff}}(\phi, T)$.
- Usually at high T, $v \to 0$ due to thermal effects [Kirzhnitz, 1972] (symmetry restoration).
- As the universe cools, there is a phase transition from $v = 0$ to $v \neq 0$.
- Order parameter: $v(T)$.

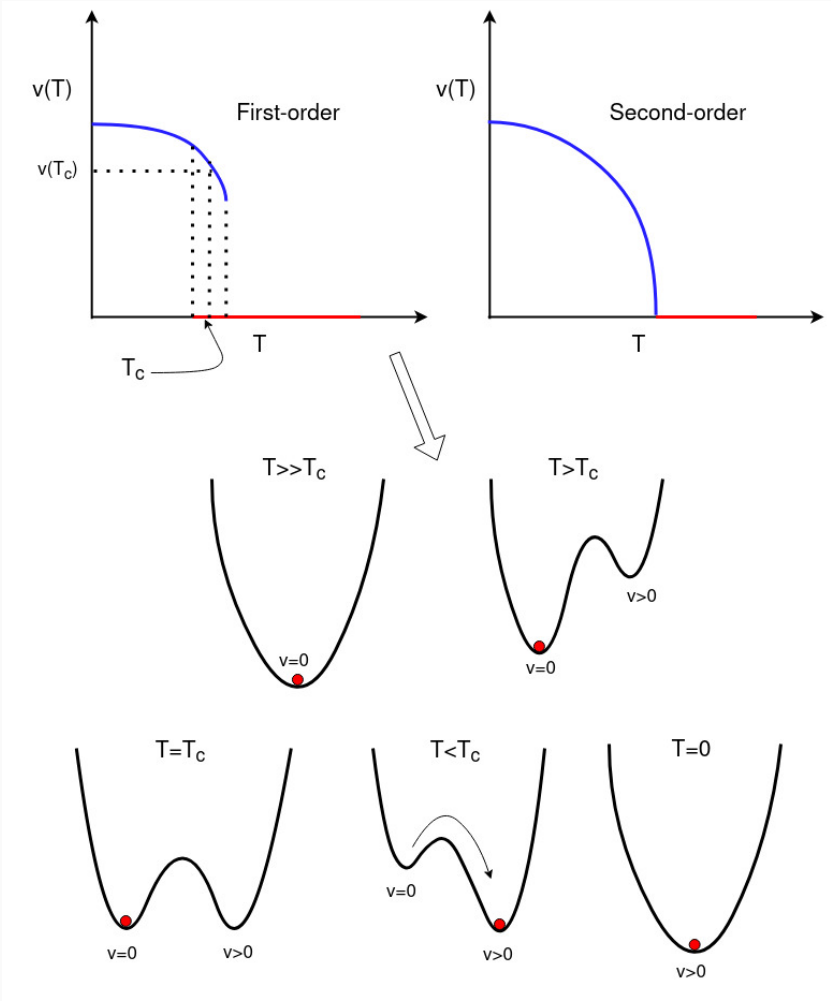

FOPT and GWs

- FOPT $\implies$ bubbles of true phase nucleate in a sea of false phase.
- Tunneling probability [Callan-Coleman 1977; Linde, 1977], $\Gamma(T) \approx T^4 \left(\frac{S_3}{2\pi T}\right)^{3/2} e^{-\frac{S_3}{T}}$.
- Strength of FOPT characterized by,
  1. T_n: $\Gamma(T_n) \sim \mathcal{O}(1)$,
  2. Ratio of latent heat and radiation density, α,
  3. Rate of PT, $\beta \equiv -\left.\frac{dS}{dt}\right|_{t=t_*} = T H_* \left.\frac{dS}{dT}\right|_{T=T_*}$.
- Bubbles expand rapidly, collide with each other.
- GWs are produced by: bubble collisions, sound waves in the plasma, and MHD turbulence. $h^2\Omega_{\rm GW} \approx h^2\Omega_{\rm coll} + h^2\Omega_{\rm sw} + h^2\Omega_{\rm turb}$.
- Large α, small β/H_* $\implies$ strong FOPT $\implies$ strong GW background.
- $f_{\rm peak} \propto T_n$.

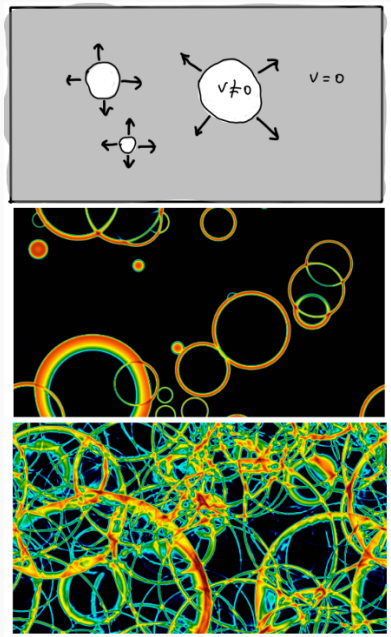

[D. Weir, 2017]

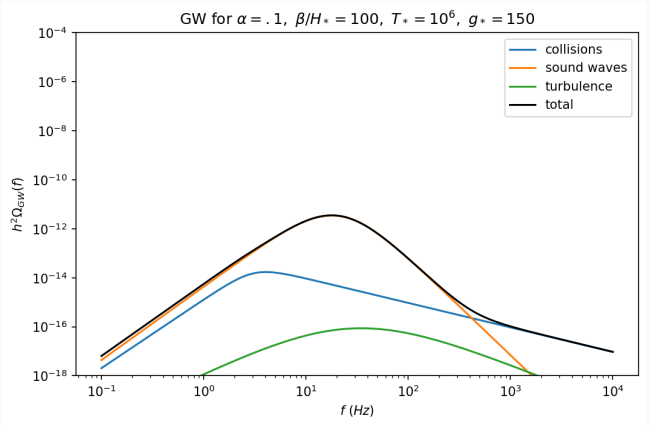

Constraining models with GWs from FOPT

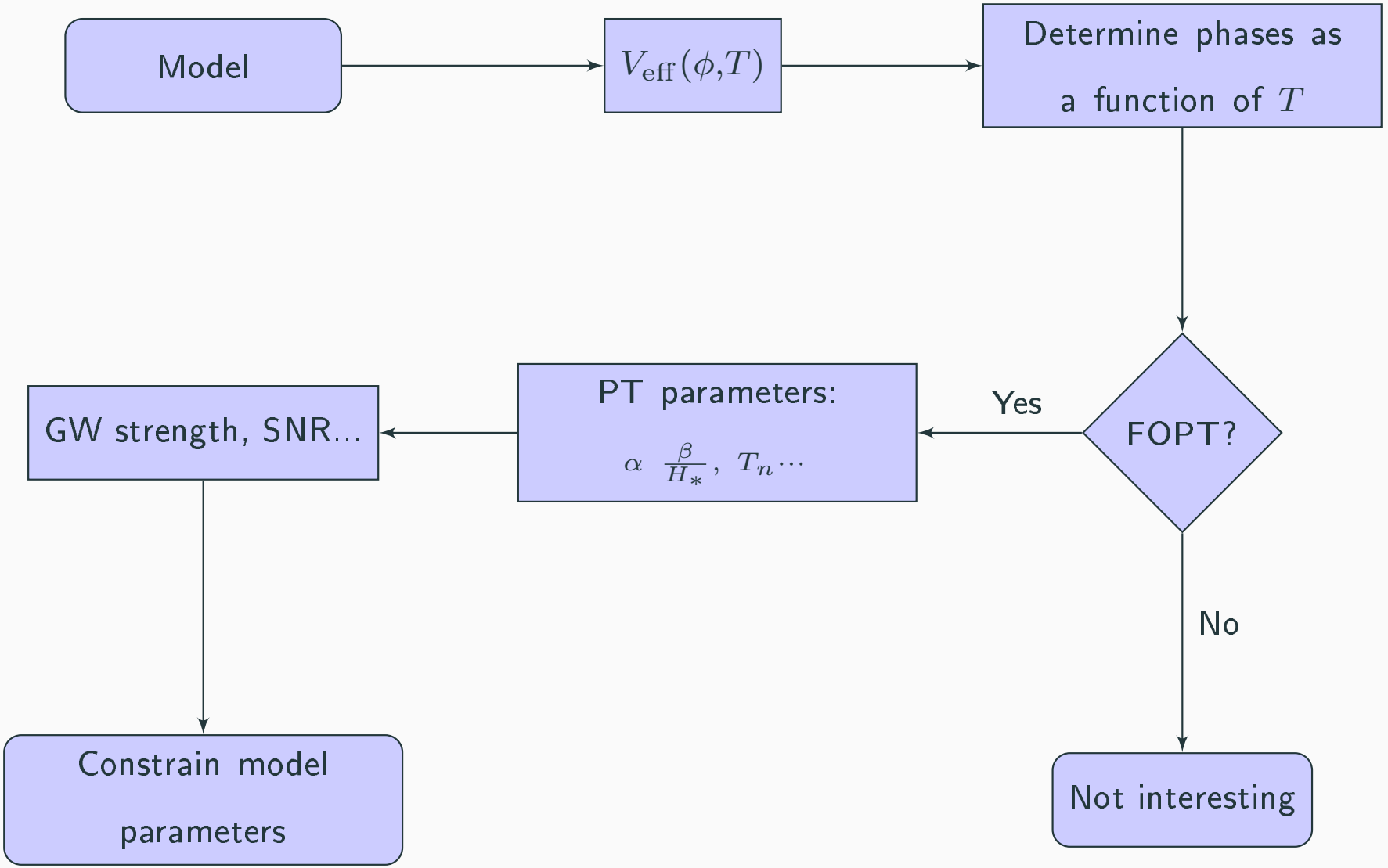

The model

Left-right symmetric model

- LRSM gauge group:

$$\mathcal{G}_{\rm LRSM} = SU(3)_c \times SU(2)_L \times SU(2)_R \times U(1)_{B-L}$$

- Breaking pattern: $\mathcal{G}_{\rm LRSM} \xrightarrow{v_R} \mathcal{G}_{\rm SM} \xrightarrow{v_L, \kappa_1, \kappa_2} U(1)_{\rm em}$
- Scalars for SSB: a bidoublet + 2 triplets (TLRSM), or a bidoublet and 2 doublets (DLRSM).
- Higgs and EWPO data: electroweak symmetry breaking in DLRSM can be much different from that in TLRSM.[1]
- For $v_R \sim \mathcal{O}(10)$ TeV, the GW background can be detected at observatories like BBO and DECIGO.

[1] Bernard et. al. 2020; Karmakar, Uma et.al. 2022

Doublet left-right symmetric model

- Fermions:

$$Q_L = \begin{pmatrix} u_L \\ d_L \end{pmatrix} \sim (3,2,1,1/3), \qquad Q_R = \begin{pmatrix} u_R \\ d_R \end{pmatrix} \sim (3,1,2,1/3),$$
$$L_L = \begin{pmatrix} \nu_L \\ e_L \end{pmatrix} \sim (1,2,1,-1), \qquad L_R = \begin{pmatrix} \nu_R \\ e_R \end{pmatrix} \sim (1,1,2,-1).$$

- Scalars:

$$\Phi = \begin{pmatrix} \phi_1^0 & \phi_2^+ \\ \phi_1^- & \phi_2^0 \end{pmatrix} \sim (1,2,2,0),$$
$$\chi_L = \begin{pmatrix} \chi_L^+ \\ \chi_L^0 \end{pmatrix} \sim (1,2,1,1), \text{ and } \chi_R = \begin{pmatrix} \chi_R^+ \\ \chi_R^0 \end{pmatrix} \sim (1,1,2,1).$$

- Yukawa lagrangian:

$$\mathcal{L}_{\rm Y} \supset -\bar{Q}_{Li}(y_{ij}\Phi + \tilde{y}_{ij}\tilde{\Phi})Q_{Rj} + \text{h.c.}$$

Talk by Prof. S. Umasankar

- Parity-symmetric scalar potential:

$$
\begin{aligned}
V &= V_2+V_3+V_4, \\
V_2 &= -\mu_1^2\mathrm{Tr}(\Phi^\dagger\Phi)-\mu_2^2\ [\mathrm{Tr}(\tilde{\Phi}\Phi^\dagger)+\mathrm{Tr}(\tilde{\Phi}^\dagger\Phi)]-\mu_3^2\ [\chi_L^\dagger\chi_L+\chi_R^\dagger\chi_R], \\
V_3 &= \mu_4\ [\chi_L^\dagger\Phi\chi_R+\chi_R^\dagger\Phi^\dagger\chi_L]+\mu_5\ [\chi_L^\dagger\tilde{\Phi}\chi_R+\chi_R^\dagger\tilde{\Phi}^\dagger\chi_L], \\
V_4 &= \lambda_1\mathrm{Tr}(\Phi^\dagger\Phi)^2+\lambda_2\ [\mathrm{Tr}(\tilde{\Phi}\Phi^\dagger)^2+\mathrm{Tr}(\tilde{\Phi}^\dagger\Phi)^2]+\lambda_3\mathrm{Tr}(\tilde{\Phi}\Phi^\dagger)\,\mathrm{Tr}(\tilde{\Phi}^\dagger\Phi) \\
&\quad +\lambda_4\mathrm{Tr}(\Phi^\dagger\Phi)\,[\mathrm{Tr}(\tilde{\Phi}\Phi^\dagger)+\mathrm{Tr}(\tilde{\Phi}^\dagger\Phi)]+\rho_1\ [(\chi_L^\dagger\chi_L)^2+(\chi_R^\dagger\chi_R)^2]+\rho_2\ \chi_L^\dagger\chi_L\chi_R^\dagger\chi_R \\
&\quad +\alpha_1\mathrm{Tr}(\Phi^\dagger\Phi)[\chi_L^\dagger\chi_L+\chi_R^\dagger\chi_R]+\left\{\alpha_2\ [\chi_L^\dagger\chi_L\mathrm{Tr}(\tilde{\Phi}\Phi^\dagger)+\chi_R^\dagger\chi_R\mathrm{Tr}(\tilde{\Phi}^\dagger\Phi)]+\mathrm{h.c.}\right\} \\
&\quad +\alpha_3\ [\chi_L^\dagger\ \Phi\Phi^\dagger\chi_L+\chi_R^\dagger\Phi^\dagger\Phi\chi_R]+\alpha_4\ [\chi_L^\dagger\ \tilde{\Phi}\tilde{\Phi}^\dagger\chi_L+\chi_R^\dagger\tilde{\Phi}^\dagger\tilde{\Phi}\chi_R],
\end{aligned}
$$

- $\langle\Phi\rangle = \frac{1}{\sqrt{2}}\begin{pmatrix}\kappa_1 & 0\\ 0 & \kappa_2\end{pmatrix},\ \langle\chi_L\rangle = \frac{1}{\sqrt{2}}\begin{pmatrix}0\\ v_L\end{pmatrix},\ \langle\chi_R\rangle = \frac{1}{\sqrt{2}}\begin{pmatrix}0\\ v_R\end{pmatrix}.$
- Introduce: $r \equiv \frac{\kappa_2}{\kappa_1},\ w \equiv \frac{v_L}{\kappa_1}$.
- Parameter set: $\{\lambda_{1,2,3,4},\ \alpha_{1,2,3,4},\ \rho_{1,2},\ \mu_4,\ r,\ w,\ v_R\}$.

Particle spectrum

Sector	Label
CP-even scalars	h, H_1, H_2, H_3
CP-odd scalars	A_1, A_2
Charged scalars	$H_1^{\pm}, H_2^{\pm}$
Charged gauge bosons	$W_{1\mu}^{\pm}, W_{2\mu}^{\pm}$
Neutral gauge bosons	$A_\mu, Z_{1\mu}, Z_{2\mu}$

- SM Higgs: $m^2_{h,\text{analytic}} \approx v^2 \left(2\lambda_1 - \frac{(\alpha_1+\alpha_4)^2}{2\rho_1} \right)$.
- Other scalars:

$$m^2_{H_1} \simeq m^2_{A_1} \simeq m^2_{H_1^{\pm}} \approx \tfrac{1}{2}(\alpha_3 - \alpha_4) v_R^2 \,,$$
$$m^2_{H_2} \simeq m^2_{A_2} \simeq m^2_{H_2^{\pm}} \approx \tfrac{1}{2}(\rho_2 - 2\rho_1) v_R^2 \,,$$
$$m^2_{H_3} = 2\rho_1 v_R^2 \,,\; m^2_{H_2} > m^2_{H_1} \,.$$

- Gauge bosons: $m_{W_1} = m_W$, $m_{Z_1} = m_Z$, and $m_{W_2, Z_2} \sim \mathcal{O}(v_R)$.

Phenomenological constraints

- Theoretical bounds: perturbativity, unitarity, bounded from below.
- Recent bound on W_2 mass: $m_{W_2} > 5.1\,\text{TeV}$. [Pich et. al. 2023]
- This gives[2] $v_R > \frac{2m_{W_2}}{g} = 15.7\,\text{TeV}$.
- $hb\bar{b}$ coupling rules out large parameter space, $\kappa_b = 0.98^{+0.14}_{-0.13}$.
- Neutral meson mixing constraint: $m_{H_1} > 15\,\text{TeV}$. [Zhang et. al. 2008]
- Trilinear higgs coupling: ATLAS bound, $\kappa_h = \frac{c_{h^3}}{c_{h^3}^{\text{SM}}} \in [-2.3, 10.3]$ at 95% CL.

[2] we take $g_L = g_R = g$

$SU(2)_R \times U(1)_{B-L}$ breaking phase transition

Parameter scan

- For $SU(2)_R \times U(1)_{B-L}$ breaking PT, $V_{\rm eff} \equiv V_{\rm eff}(R, T)$.
- $V_{\rm eff}(R, T) = V_0 + V_{\rm CW} + V_{\rm c.t.} + V_{1T} + V_{\rm Daisy}$
- 'Simple basis': $\lambda_0 \equiv \lambda_1 = \lambda_3 = \lambda_4,\ \lambda_2,\ \alpha_0 \equiv \alpha_1 = \alpha_2 = \alpha_4$.
- Parameter set: $\{\lambda_0,\ \alpha_0,\ \rho_1,\ \rho_2,\ r,\ w.\ v_R\}$.

$$\log \alpha_0 \in [-3, 0],\ \log \alpha_3 \in [-3, 0],\ \log \rho_1 \in [-3.5, -0.5],$$
$$\rho_2 \in [0, 4\pi],\ x \equiv \frac{\lambda_2}{\lambda_0} \in [0.25, 0.85],\ \log r \in [-3, 0],$$
$$\log w \in [-6, 1],\ v_R = 20,\ 30,\ 50\,\text{TeV}.$$

- Filter points using theoretical and experimental bounds.
- Look for FOPT.[3] SFOPT condition: $\xi_c \equiv \frac{v_c}{T_c} > 1$.
- For points with SFOPT, compute: $\alpha,\ \beta/H_*,\ T_n$.

[3] We used a modified version of `CosmoTransitions`.

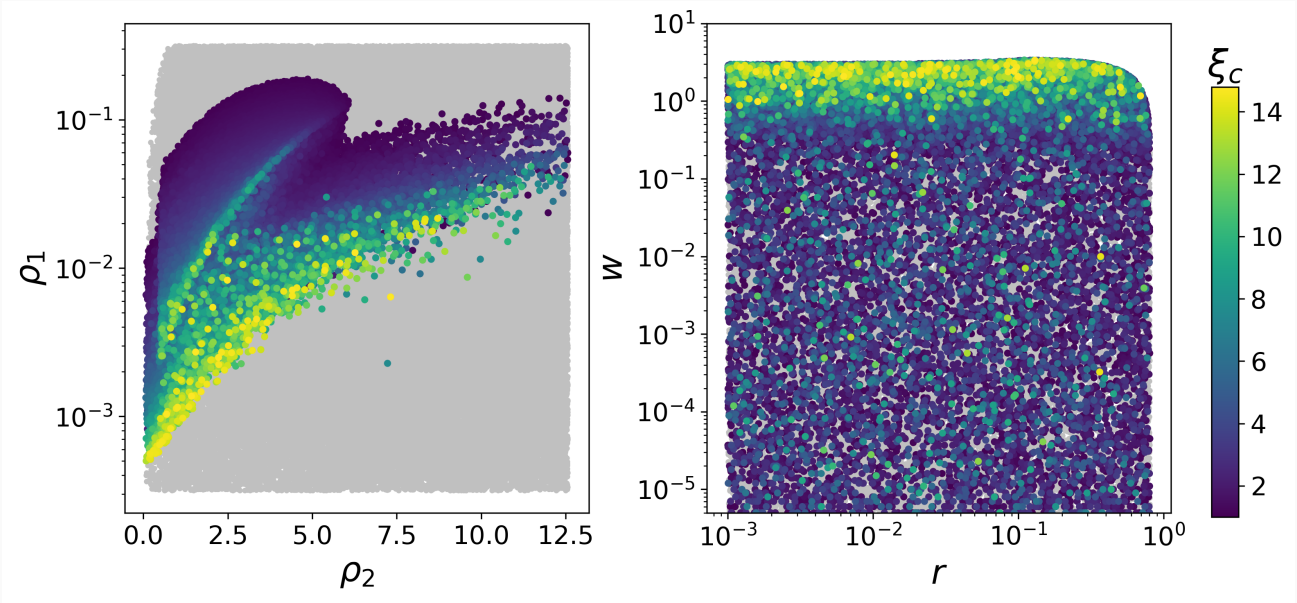

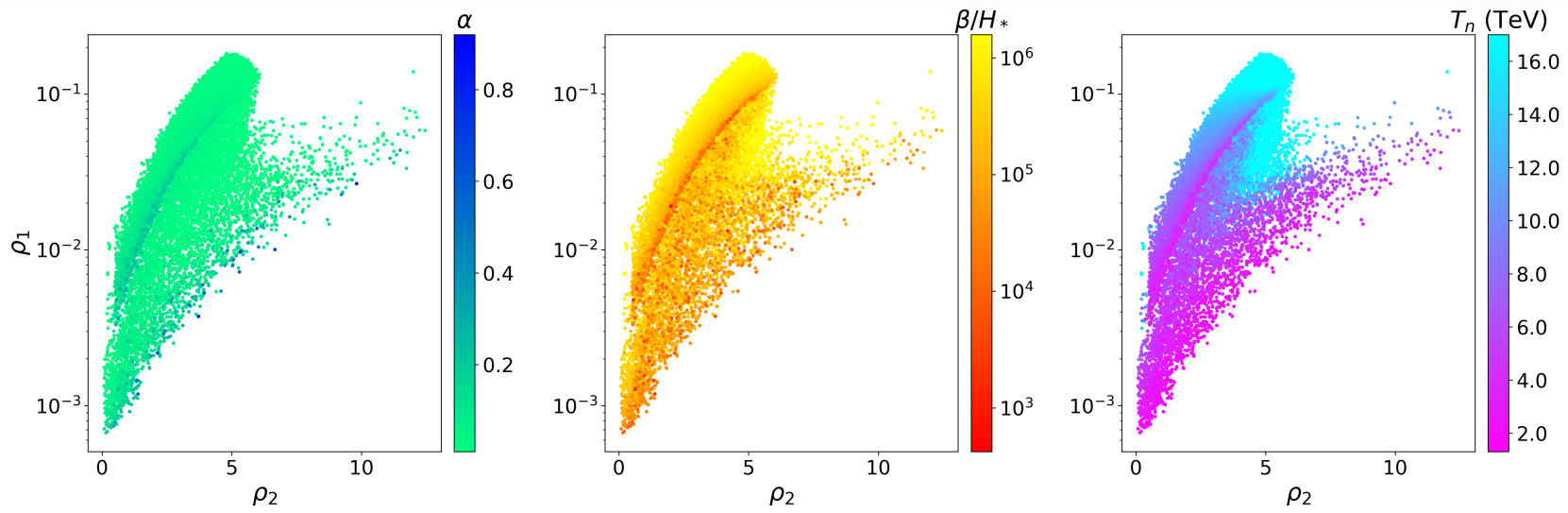

Variation of PT parameters, $v_R = 30$ TeV. SFOPT is for small ρ_1, and $w \sim \mathcal{O}(1)$.

Gravitational wave background

GW spectra

- Non-runaway scenario: $h^2\Omega_{\rm GW} \approx h^2\Omega_{\rm sw} + h^2\Omega_{\rm turb}$.
- Terminal bubble wall velocity, $v_w \approx 1$.
- $\Omega_{\rm GW}(f_{\rm peak}) \propto v_w \left(\frac{H_*}{\beta}\right)^x \left(\frac{\kappa\alpha}{1+\alpha}\right)^y \left(\frac{100}{g_*}\right)^{1/3}$, where $x, y > 0$, κ efficiency factor.

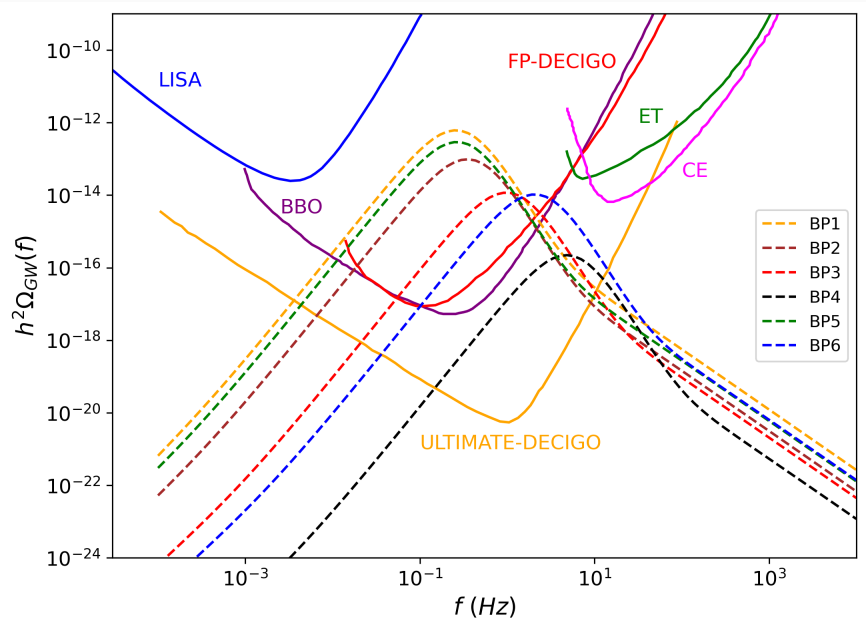

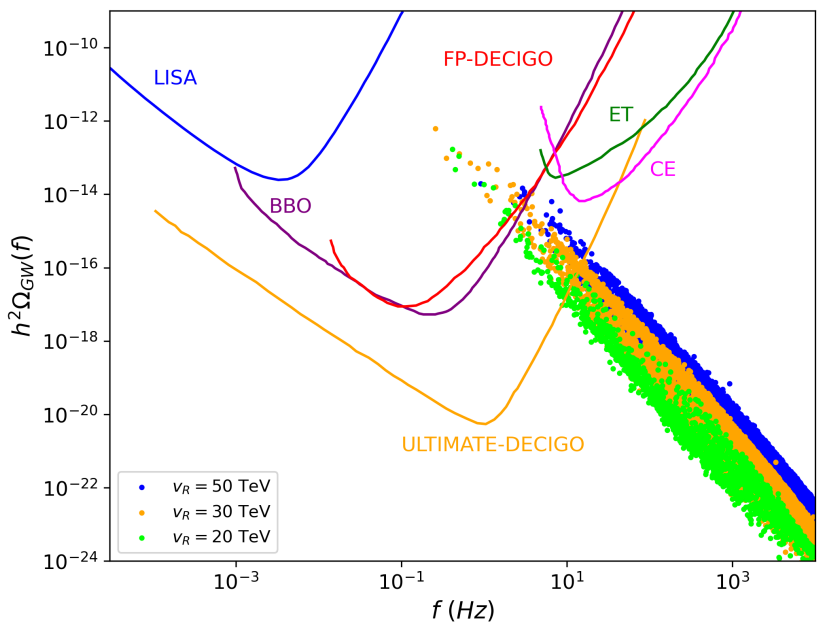

Left: GW spectra for 6 benchmark points. Right: $v_R = 20,\ 30$, and 50 TeV.

Outlook

Collider signatures

- GW favours $\rho_1 \lesssim \mathcal{O}(10^{-1})$, i.e. light H_3.
- FCC-hh at $\sqrt{s} = 100\,\text{TeV}$ with $\sigma \sim \mathcal{O}(fb)$ can rule out m_{H_3} upto $2\,\text{TeV}$. [DeV, 2016]
- HE-LHC, CLIC_{3000}, and FCC-hh will improve sensitivity of κ_h to $\sim 20\%, 10\%$, and 5% respectively.

$\delta\kappa_h$	20 TeV	30 TeV	50 TeV
$> 5\%$	52%	58%	50%
$> 10\%$	21%	34%	33%
$> 20\%$	8%	20%	25%

Percentage of points detectable at Ultimate-DECIGO

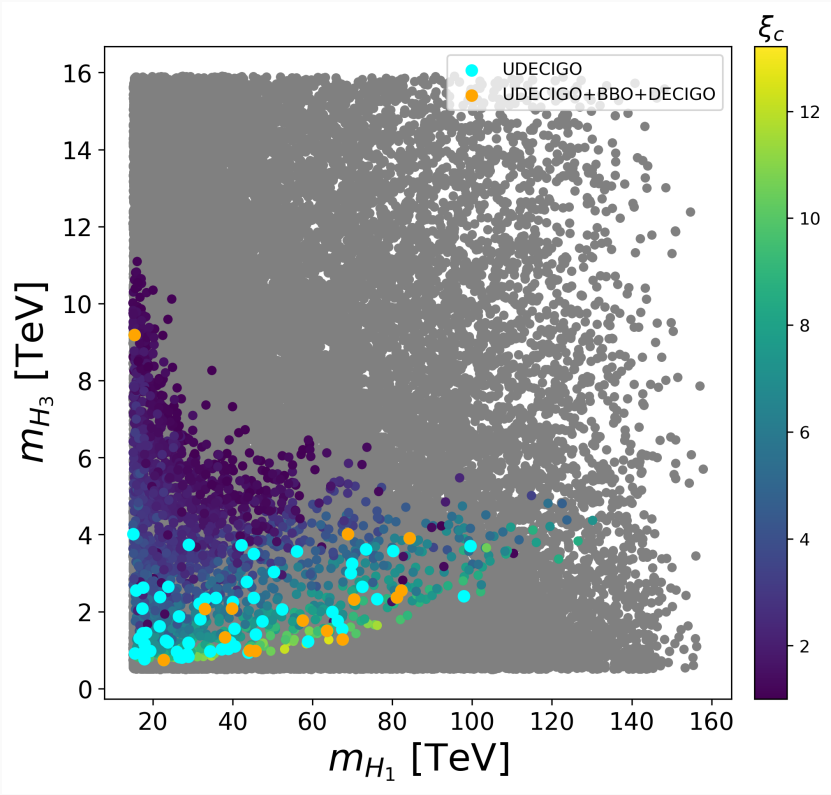

Detectable points for $v_R = 20\,\text{TeV}$

Conclusions

- GWs are a promising window to the early universe.
- GWs from $SU(2)_R \times U(1)_{B-L}$ PT, possibly detectable at BBO, FP-DECIGO, Ultimate-DECIGO, for $v_R = 20,\ 30,\ 50\,\text{TeV}$.
- Preference for a light H_3. Future colliders will be able to rule out m_{H_3} upto a few TeV.
- Preference for $w \sim \mathcal{O}(1) \implies$ pattern of EWSB is different from TLRSM.
- Complementary collider probes for light H_3, and $\delta\kappa_h$.

Thank You!

Effective potential

- Background field value of the neutral CP-even field, χ^0_{Rr}: R.
- For $SU(2)_R \times U(1)_{B-L}$ breaking PT, $V_{\rm eff} \equiv V_{\rm eff}(R,T)$.
- The effective potential is,

$$
\begin{aligned}
V_{\rm eff}(R,T) &= V_0 + V_{\rm CW} + V_{\rm c.t.} + V_{1T} + V_{\rm Daisy} \\
V_0(R) &= -\frac{\mu_3^2}{2} R^2 + \frac{\rho_1}{4} R^4, \\
V_{\rm CW}(R) &= \frac{1}{64\pi^2} \sum_i (-1)^{f_i} n_i m_i^4(R) \left[\log\left(\frac{m_i^2(R)}{\mu^2} \right) - c_i \right], \\
V_{1T}(R,T) &= \frac{T^4}{2\pi^2} \sum_i (-1)^{f_i} n_i J_{b/f}\left(\frac{m_i^2}{T^2} \right), \\
V_{\rm Daisy} &= -\frac{T}{12\pi} \sum_i n_i \left((m_i^2(R) + \Pi_i(T))^{3/2} - (m_i^2(R))^{3/2} \right).
\end{aligned}
$$

- $V_{\rm c.t.}$ is chosen such that the one-loop *vev* and mass coincide with the tree-level values.

Large T expansion of V_{1T}

$$J_{b/f}(x^2) = \pm \int_0^\infty dy\; y^2 \log\left(1 \mp e^{-\sqrt{x^2+y^2}}\right).$$

For small x^2,

$$\begin{aligned}
J_f(x^2,n) = &- \frac{7\pi^4}{360} + \frac{\pi^2}{24}x^2 + \frac{1}{32}x^4\left(\log x^2 - c_f\right) \\
&- \pi^2 x^2 \sum_{l=2}^{n} \left(-\frac{1}{4\pi^2}x^2\right)^l \frac{(2l-3)!!\zeta(2l-1)}{(2l)!!(l+1)}\left(2^{2l-1}-1\right), \\
J_b(x^2,n) = &- \frac{\pi^4}{45} + \frac{\pi^2}{12}x^2 - \frac{\pi}{6}\left(x^2\right)^{3/2} - \frac{1}{32}x^4\left(\log x^2 - c_b\right) \\
&+ \pi^2 x^2 \sum_{l=2}^{n} \left(-\frac{1}{4\pi^2}x^2\right)^l \frac{(2l-3)!!\zeta(2l-1)}{(2l)!!(l+1)}.
\end{aligned}$$

Small T expansion of V_{1T}

For large x^2, both fermions and bosons have the same expansion,

$$J_{b/f}(x^2,n)=-\exp\left(-(x^2)^{1/2}\right)\left(\frac{\pi}{2}(x^2)^{3/2}\right)^{1/2}\sum_{l=0}^{n}\frac{1}{2^l\,l!}\frac{\Gamma(5/2+l)}{\Gamma(5/2-l)}(x^2)^{-l/2}.$$

Daisy Resummation

- Particles receive thermal (Debye mass) due to 'hard loops'[4]. Scalars, longitudinal component of gauge bosons and fermions get thermal mass. For $SU(N)$,

$$\Pi^L = g_N^2 T^2 \left[\frac{N}{3} + \frac{1}{6} \sum_s n_s C(r_s) + \frac{1}{12} \sum_f n_f C(r_f) \right].$$

- For N-loop diagrams with $N-1$ petals, $\Pi_{\text{daisy}} \sim \lambda^N \frac{T^{2N-1}}{\mu^{2N-3}}$.
- Breakdown of perturbativity: At $T_c \sim \frac{\mu}{\sqrt{\lambda}}$, parameter $\alpha \equiv \lambda \frac{T^2}{\mu^2} \sim 1$.
- Resummed contribution from daisy diagrams $\implies m^2 \to m^2 + \Pi(T)$.
- Effect is to shift $V_T \to V_T + V_{\text{daisy}}$.
- Generally, perturbation theory can be applied is $\frac{\phi_c}{T_c} \gtrsim 1$.

[4] Thesis-Breitbach, 2018

Other projections

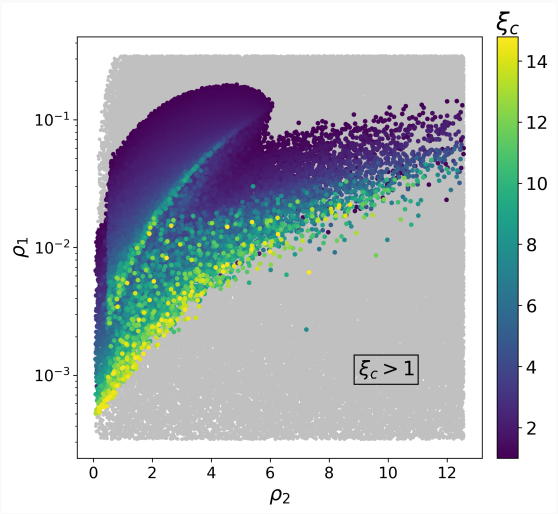

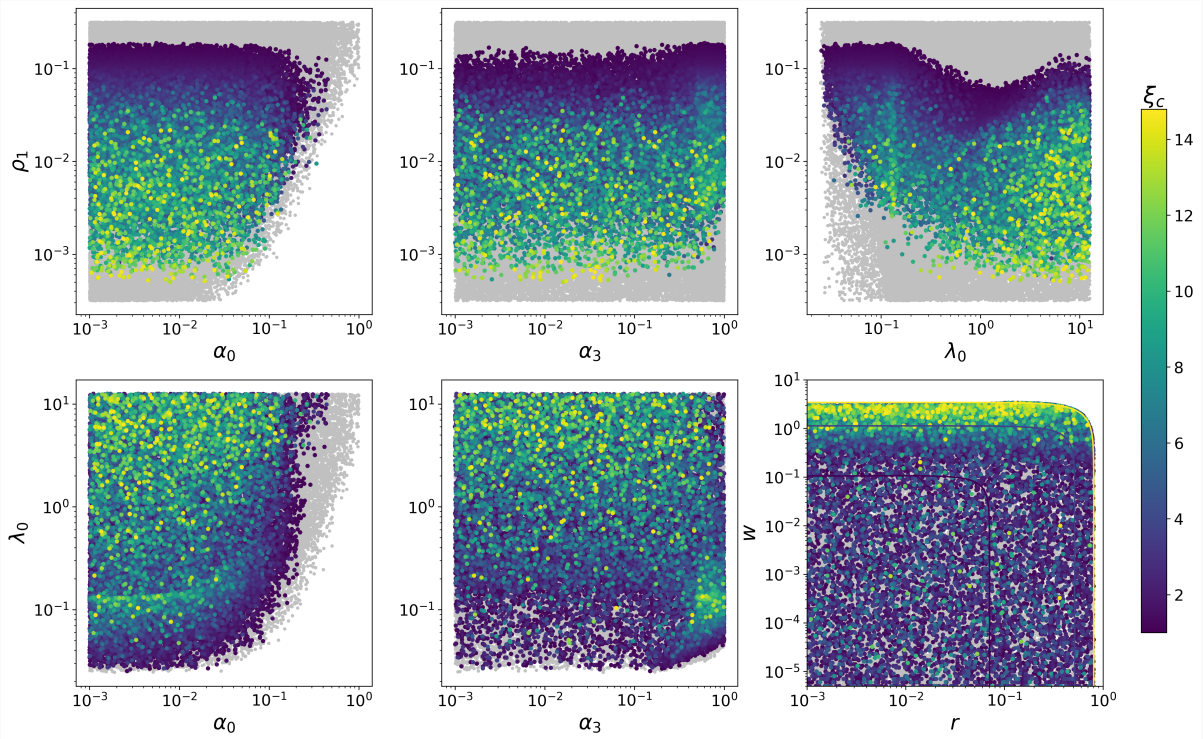

GW Detection

- For detection time t, $\mathrm{SNR} = \sqrt{\tau \int_{f_{\min}}^{f_{\max}} df \left[\frac{\Omega_{\mathrm{GW}}(f)h^2}{\Omega_{\mathrm{sens}}(f)h^2}\right]^2}$
- Signal is detectable if $\mathrm{SNR} > \mathrm{SNR}_{\mathrm{thr}}$.
- Six BPs were identified with high SNR at BBO, FP-DECIGO and Ultimate DECIGO.

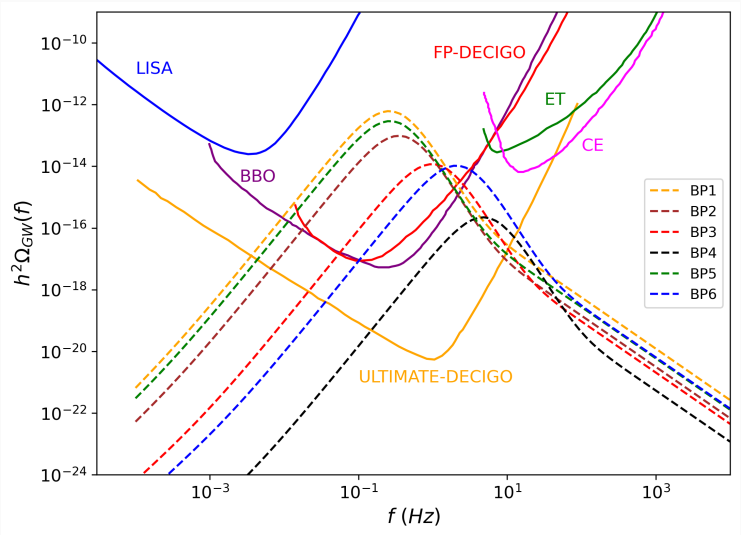

GW spectra for the benchmark points

Detectable points in the $r - w$ plane

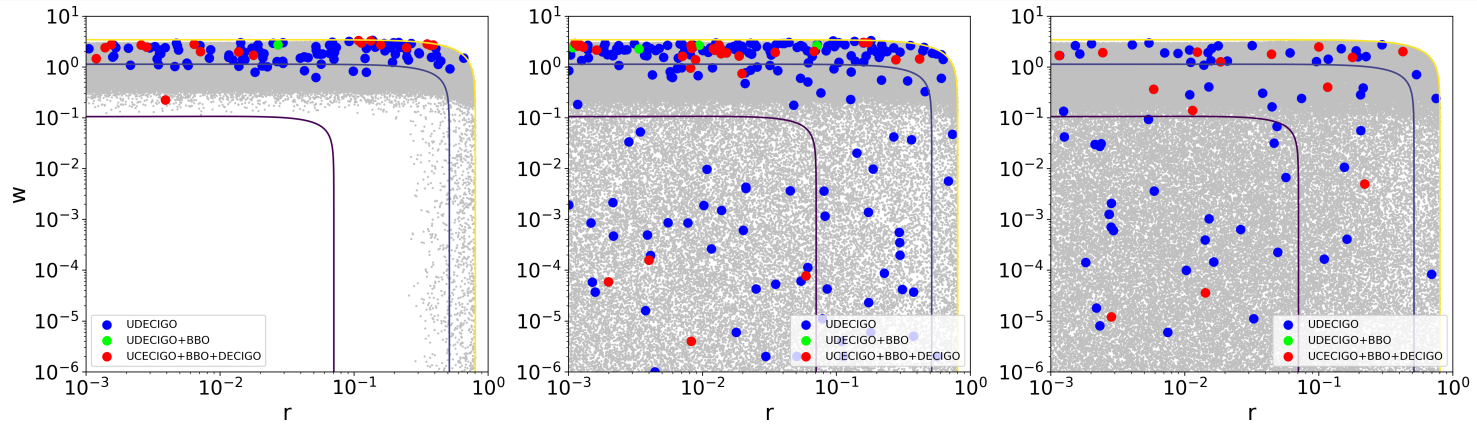

GW spectra for the benchmark points

H_3 production channels:

1. H_1-decay, $pp \to H_1 \to hH_3$,
2. decay of boosted h, $pp \to h^* \to hH_3, H_3H_3$,
3. Higgsstrahlung, $pp \to V_R^* \to V_R H_3$,
4. $V_R V_R$ fusion, $pp \to H_3 jj$.